Available online at www.sciencedirect.com
SCIENCE DIRECT®
Journal of Chromatography A, 1040 (2004) 63–72
JOURNAL OF CHROMATOGRAPHY A
www.elsevier.com/locate/chroma

Countercurrent chromatographic separation: a hydrodynamic approach developed for extraction columns

A.E. Kostanian [a], A. Berthod [b,*], S.N. Ignatova [c], T.A. Maryutina [c], B.Ya. Spivakov [c], I.A. Sutherland [d]

[a] *Kurnakov Institute of General and Inorganic Chemistry, Russian Academy of Sciences, Leninsky Prosp. 31, Moscow 117907, Russia*
[b] *Laboratoire des Sciences Analytiques, Université Claude-Bernard, Lyon 1, UMR CNRS 5180, Bat. CPE-308, Villeurbanne Cedex 69622, France*
[c] *Vernadsky Institute of Geochemistry and Analytical Chemistry, Russian Academy of Sciences, Kosygin St. 19, Moscow 119991, Russia*
[d] *Brunel Institute for Bioengineering, Brunel University, Uxbridge UB8 3PH, UK*

Received 16 January 2004; received in revised form 29 March 2004; accepted 29 March 2004

Abstract

In countercurrent chromatography (CCC) both stationary and mobile liquids undergo intense mixing in the variable force field of a coil planet centrifuge and the separation process, like the separation in conventional solvent extraction column, is influenced by longitudinal mixing in the phases and mass transfer between them. This paper describes how the residence time distribution (or the elution profile) of a solute in CCC devices and the interpretation of experimental peaks, can be described by a recently developed cell model of longitudinal mixing. The model considers a CCC column as a cascade of perfectly mixed equal-size cells, the number of which is determined by the rates of longitudinal mixing in the stationary and mobile phases. Experiments were carried out to demonstrate the validation of the model and the possibility of predicting the partitioning behaviour of the solutes. The methods for estimating model parameters are discussed. Longitudinal mixing rates in stationary and mobile phases have been experimentally determined and experimental elution profiles are compared with simulated peaks. It is shown that using the cell model the peak shape for a solute with a given distribution constant can be predicted from experimental data on other solutes.

Keywords: Longitudinal dispersion; Countercurrent chromatography; Mathematical modelling; Extraction columns

1. Introduction

Countercurrent chromatography (CCC), a form of liquid–liquid chromatography without a solid support, combines the features of liquid–liquid extraction and partition chromatography [1–6]. It is applied to analytical and preparative scale separations of chemical and pharmaceutical substances. For scaling up, optimisation of device design and operation parameters of CCC, further development of the theory of CCC separation processes is necessary. It is important to find an appropriate mathematical function, which could describe the peak shapes. A large number of empirical functions are known and used for the description and interpretation of chromatographic peaks [7]. As a rule, the parameters of these mathematical functions are not directly related to a real chromatographic process and their application for the scaling up of a device is problematic. For the reliable simulation and scale up, the mathematical model used must be able to reflect, even in a simplified form, the characteristic features of a solute spreading mechanism in a chromatographic tubing.

A cell model of the chromatographic process that takes into account longitudinal mixing in both phases has been developed [8], on the basis of the approaches used in chemical engineering for modelling of mass transfer processes, in particular solvent extraction columns.

1.1. CCC devices and extraction columns

The chromatographic column can be considered as a very long extraction column with an extremely high length to diameter ratio, operating under special conditions; one of the phases is held stationary and the process is running under non-steady state conditions. Extraction columns are

* Corresponding author. Tel.: +33-472-431434; fax: +33-472-431078.
E-mail address: berthod@univ-lyon1.fr (A. Berthod).

0021-9673/$ – see front matter © 2004 Published by Elsevier B.V.
doi:10.1016/j.chroma.2004.03.055

normally devices in which light and heavy phases move countercurrently through a vertical cylindrical vessel, operating under steady-state conditions. Columns in common use can be divided into two general groups:

1. Intensified columns using energy input to provide a high degree of contact between the two phases (rotating disk or impeller columns, pulsed columns with sieves or packing, vibrating plate columns).
2. Columns without energy input (spray columns, packed columns, plate columns).

CCC devices belong to the first group: interphase mass transfer is enhanced by energy supply due to the centrifugal force field produced by the rotation of the coil planet centrifuge. A sufficient interfacial area should be provided in chromatographic tubing so that the mass transfer would be reasonably rapid.

The process in both devices (extraction column and chromatographic tubing) is influenced by interphase mass transfer and longitudinal dispersion of the solute caused by axial mixing in the phases. There can be two limiting cases under consideration:

1. The mass transfer governs the process. For the stationary phase retention $S_f > 0.5$, a rotation speed increase will increase the number of mixing and settling cycles per unit time, but will also increase the "g" field, which can have an inhibiting effect on wave mixing. An increase in flow rate will also increase the interfacial area (due to the increase of mobile phase volume) as well as the separation (interphase mass transfer) efficiency, but up to the point where the decrease of contacting time will balance the increase of interfacial area. Both of these factors are important trade-offs which need to be understood.
2. The interphase mass transfer is rapid enough to be ignored. In other words, instantaneous equilibrium attainment is assumed, and the process is governed only by the axial dispersion of a solute in the stationary and mobile phases and the distribution constant in the solvent system employed. The process can be described on the bases of continuous or discrete (staged) models.

1.2. Description of the mathematical models of axial mixing

In conventional chromatography, it is assumed that a solute is transported along the column only with the mobile phase and remains longitudinally motionless in the stationary phase. In CCC, because of the lack of a solid support, both liquids undergo intense mixing in the variable force field of a coil planet centrifuge. The axial transport of a solute in the stationary phase, due to the reciprocal tangential acceleration vector within each individual coil segment during each rotation, can contribute considerably to the spreading of matter in the tubing.

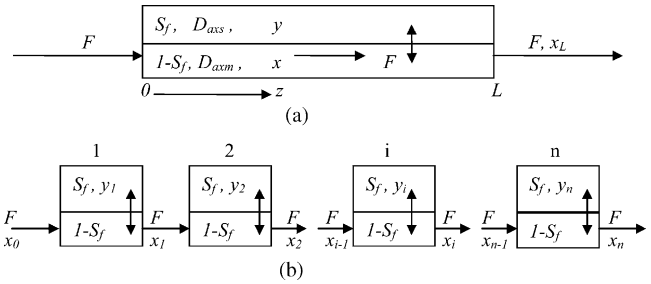

Fig. 1. Scheme of diffusion (a) and cell (b) models of CCC separation.

A continuous-diffusion model and discrete (staged) cell model (a cascade of well mixed equal-size vessels) are shown in Fig. 1. The diffusion model takes into account the rate of mixing in both phases in terms of effective longitudinal diffusion coefficients (D_{axm} in mobile phase, D_{axs} in stationary phase). In the staged model, the axial mixing in the chromatographic column is characterised by one parameter, the number of perfectly (ideally) mixed cells n.

It is assumed that:

- instantaneous equilibrium between the phases is reached at any cross-section of the continuous model and in any perfectly mixed cell of the staged model;
- the distribution constant $K_D = y/x = \text{constant}$ (here x and y are substance concentrations in mobile and stationary phases, respectively);
- the retained volume of stationary phase V_s is constant at any cross-section of the column, or when it is expressed as a fraction of column volume S_f

$$S_f = \frac{V_s}{(V_s + V_m)} = \frac{V_s}{V_c} = \text{constant}$$

where V_m and V_s are the volumes of mobile and stationary phases in the chromatographic column, respectively, and $V_c = V_s + V_m$ is the column volume.

According to Fig. 1, the equations of models have the following form:

1.2.1. Continuous model (a)

$$D_{axm}(1 - S_f)\frac{\partial^2 x}{\partial z^2} - u\frac{\partial x}{\partial z} + D_{axs}S_f\frac{\partial^2 y}{\partial z^2} = (1 - S_f)\frac{\partial x}{\partial \tau} + S_f\frac{\partial y}{\partial \tau} \quad (1)$$

$$D_{axm}(1 - S_f)\left(\frac{\partial x}{\partial z}\right)_0 + D_{axs}S_f\left(\frac{\partial y}{\partial z}\right)_0 - ux(z = 0) = 0 \quad (2)$$

$$\left(\frac{\partial x}{\partial z}\right)_L = 0 \quad (3)$$

1.2.2. Staged model (b)

$$\frac{V_m}{n}\frac{dx_i}{d\tau} + \frac{V_s}{n}\frac{dy_i}{d\tau} = Fx_{i-1} - Fx_i \quad (4)$$

with $i = 1, 2, \ldots, n$; where $u = F/A_c$ is mobile phase linear velocity related to the whole column cross-section A_c (in chromatographic terms it is the velocity of a $K_D = 1$ solute), z the longitudinal coordinate along the flow tube, F the volumetric flow rate of mobile phase and τ the time.

The boundary conditions (2) and (3) are derived from material balances at the ends of a closed channel (chromatographic tubing).

It must be noted that the models described are similar to those considered in general chromatography theory [9–13].

The solutions of Eqs. (1) and (4) with corresponding initial conditions (describing the sample injection into the system at the mobile phase inlet at the time $\tau = 0$) will give the chromatographic peak shape of a solute on the basis of the continuous and staged (cell) models. In normalised form these functions will describe the residence time distributions of a solute in a chromatographic column.

The rigorous solution of Eq. (1) with boundary conditions (2) and (3) is very complicated and not well suited for practical use. For low degree of longitudinal mixing the solution of diffusion model equation can be approximated by a normal (Gaussian) distribution:

$$\frac{x_L}{\bar{x}} = \frac{p}{2\sqrt{\pi/Pe}}\exp\left[-\frac{(1-pt)^2 Pe}{4}\right] = \frac{V_c/V_R}{2\sqrt{\pi/Pe}}\exp\left[-\frac{(1-\tau/\tau_R)^2 Pe}{4}\right] \quad (5)$$

with

$$Pe = \frac{uL}{(1-S_f)D_{axm} + K_D S_f D_{axs}} \quad (6)$$

and

$$p = \frac{1}{1 - S_f + S_f K_D} = \frac{V_c}{V_R} \quad (7)$$

where $\bar{x} = Q/V_c$ is the mean concentration in the column; $t = \tau(F/V_c) = (\tau_u/L) = (\tau/\tau_c)$ is the dimensionless time, $\tau_c = \tau_{K_D=1} = (V_c/F) = (L/u)$ is the mean residence time of a solute with a distribution constant of $K_D = 1$ or the mean residence time of the mobile phase in the column when $S_f = 0$, $\tau_R = V_R/F$ is the solute retention time; $V_R = V_m + K_D V_s$ is the total retention volume and is the amount of the solute in the sample injected.

The dimensionless mixing parameter Pe is known as the Peclet number. It denotes the overall axial mixing (solute spreading) rate in a chromatographic column. According to Eq. (6), the axial dispersion coefficient of the moving band is $D_{ax} = (1 - S_f)D_{axm} + K_D S_f D_{axs}$.

The solution of the set of n Eq. (4) with the following boundary and initial conditions:

$$x_0 = 0, \quad \tau = 0, \quad x_1 = \frac{nQ}{V_c(1 - S_f + S_f K_D)},$$
$$x_2 = x_3 = \cdots = x_n = 0,$$

(the primary concentration of solute in the mobile phase flow is zero; at $\tau = 0$ the amount Q of the solute in the sample is injected as a bolus into the first ideally mixed cell) is as follows [8]:

$$X = \frac{x_n}{\bar{x}} = \frac{n^n}{(n-1)!}p^n t^{n-1}\exp(-npt) = \frac{n^n}{(n-1)!}\left(\frac{\tau}{\tau_R}\right)^n \frac{V_c}{\tau F}\exp\left(-n\frac{\tau}{\tau_R}\right) \quad (8)$$

Eq. (8) describes the residence (retention-in chromatographic terms) time distribution of a solute in a chromatographic column on the basis of the cell model under equilibrium conditions. For a large number of cells n (low degree of axial mixing) the distribution function (8), as in the case of the diffusion model, can be approximated by a normal distribution:

$$X = \frac{x_n}{\bar{x}} = \frac{p}{\sqrt{2\pi/n}}\exp\left[-\frac{(1-pt)^2 n}{2}\right] \quad (9)$$

From Eqs. (5) and (9) a relationship between the parameters of the continuous and staged models can be found [8]:

$$n = \frac{Pe}{2} = \frac{n_c}{1 + S_f(\lambda - 1)} \quad (10)$$

where $n_c = (uL/2D_{axm})$ is the number of perfectly mixed cells in the mobile phase for the case $S_f = 0$; $\lambda = (K_D D_{axs}/D_{axm}) = (D_{axs}y/D_{axm}x)$ is a dimensionless number, characterising the ratio of matter dispersion in stationary phase to that in the mobile phase.

1.3. Stationary phase retention in CCC devices and dispersed phase holdup in extraction columns

Ito and coworkers [14] have established the relationship between stationary phase retention and the square root of mobile phase flow:

$$S_f = 1 - BF^{0.5} \quad (11)$$

In modelling of extraction columns, the relationship between the dispersed phase holdup S_d (fractional volume of extraction column occupied by dispersed phase) and the flow rates of continuous F_c and dispersed F_d phases is expressed by [15]:

$$\frac{F_c}{A_c(1 - S_d)} + \frac{F_d}{A_c S_d} = (1 - S_d)v_0 \quad (12)$$

where v_0 is the characteristic droplet velocity defined as the limiting velocity of droplets when $F_c = 0$ and $F_d \to 0$.

The term on the left side of Eq. (12) represents the relative velocity of the phases-the so-called “slip” velocity.

2. Theory

2.1. Axial mixing in the phases

The model of theoretical plates in classical chromatography predicts a Gaussian (normal) residence time distribution.

The number of theoretical plates is considered to be constant for all the solutes contained in a sample. The last assumption is valid when the transport of a solute along the column axis takes place only in the mobile phase. In fact, Eq. (10) demonstrates that the number of ideally mixed cells under equilibrium conditions may be different for solutes contained in a sample. This equation can be rewritten as:

$$n = \frac{uL}{2((1 - S_f)D_{axm} + K_D S_f D_{axs})} \tag{13}$$

when $D_{axs} = 0$, or more generally $(1 - S_f)D_{axm} \gg K_D S_f D_{axs}$ Eq. (13) reduces to:

$$n = \frac{uL}{2(1 - S_f)D_{axm}} \tag{14}$$

and as a result, n is independent on the distribution constant K_D and constant for all the solutes of the injected sample. This case corresponds to HPLC with a solid stationary phase.

Consider another limiting case:

$$(1 - S_f)D_{axm} \ll K_D S_f D_{axs}$$

Eq. (13) then reduces to:

$$n = \frac{uL}{2K_D S_f D_{axs}} \tag{15}$$

In this case, the ratio of cell numbers for two solutes with K_{D1} and K_{D2} is a reciprocal of their distribution constants:

$$\frac{n_1}{n_2} = \frac{K_{D2}}{K_{D1}} \tag{16}$$

It is to mention that K_D is a physicochemical parameter depending on the solute and liquid system used, whereas D_{axm} and D_{axs} are operating parameters depending mainly on process regime (rotation speed and flow rate) and apparatus scale (turbine diameter).

Rearranging Eq. (13) gives a linear relationship between the distribution constant and the inverse value of the number of ideally mixed cells for the solutes contained in a sample:

$$\frac{1}{n} = \frac{2(1 - S_f)D_{axm}}{uL} + \frac{2S_f D_{axs}}{uL} K_D \tag{17}$$

Plotting the inverse value of cell number against the distribution constant, as in Eq. (17), enables an estimation of longitudinal mixing coefficients in mobile and stationary phases to be made from the known volume retention factor for the stationary phase S_f and from the measurements of n and K_D for different solutes of a sample taken directly from chromatograms. The y-intercept $2(1 - S_f)D_{axm}/(uL)$ gives the value of D_{axm} and the slope $2S_f D_{axm}/(uL)$ gives the value of D_{axs}.

In classical chromatography the distribution constant of a solute is calculated from the elution time τ_R:

$$K_D = \frac{(\tau_R - \tau_m)V_m}{\tau_m V_s} = \frac{(\tau_R - \tau_m)(1 - S_f)}{\tau_m S_f} \tag{18}$$

where $\tau_m = \tau_{K_D=0} = V_m/F$ is the elution time of the solvent front peak.

It can be shown [8] that the time of peak maximum, τ_{max}, and the mean residence (or retention) time of a solute in the column (defined as $\bar{\tau}$) are generally different values (in chromatography practice, usually $n \geq 100$–200 and τ_{max} and $\bar{\tau}$ differ by a very small percentage). The mean residence time can be calculated from the chromatographic curve as its first moment:

$$\bar{\tau} = \frac{\int_0^\infty \tau x d\tau}{\int_0^\infty x d\tau} \approx \frac{\sum_1^m x_i \tau_i}{\sum_1^m x_i} \tag{19}$$

For both, the diffusion and cell models the expression for $\bar{\tau}$ can be obtained from the model equation as follows:

$$\bar{\tau} = \frac{\tau_c}{p} = \frac{V_c}{F}(1 - S_f + K_D S_f) \tag{20}$$

For experimental estimation of the distribution constant it is appropriate to determine K_D from the whole chromatographic curve using Eqs. (19) and (20):

$$K_D = \frac{\bar{\tau} F}{V_c S_f} - \frac{1 - S_f}{S_f} \tag{21}$$

The main advantage of using formula (21) is that the expression for the mean residence time (20) is valid for a non-equilibrium assumption as well. It is to note that Eqs. (18) and (21) are identical except for $\tau_R = \tau_{max}$ and $\bar{\tau}$ is determined by Eq. (19).

The number of theoretical plates in classical chromatography (the number of ideally mixed cells—in this paper) is usually estimated by the equation:

$$n = 16\left(\frac{\tau_R}{W_b}\right)^2 \tag{22}$$

where W_b is the base width of a peak. It is more reliable and convenient to calculate n from maximum peak height $(x_n/\bar{x})_{max}$ [8]:

$$n = 2\pi\left(\tau_{max}\frac{x_{max}}{\Delta\tau\sum_1^m x_i}\right)^2 \tag{23}$$

As will be demonstrated below this method of estimating n is less susceptible to experimental errors.

2.2. Stationary phase retention

It is well known that the mass transfer rate between the phases is proportional to the specific interfacial area (interfacial area per unite volume of liquid mixture). In mixing of two liquid phases, as a rule, one of them (dispersed phase) is being dispersed into the other (continuous phase) in form of small droplets. That is a common way in extraction to create a large specific interfacial area needed for rapid mass transfer. Assuming that the instantaneous equilibrium attainment in CCC is due to a very large interfacial area of emulsion formed in mixing cycles, there are two situations to be considered:

1. The stationary phase is dispersed into small droplets in mixing cycles.

   Applying Eq. (12) we have $S_d = S_f$, $F_c = F$, $F_d = 0$ and

$$\frac{F}{A_c(1-S_f)} = (1-S_f)v_0 \quad \text{or}$$
$$S_f = 1 - (A_c v_0)^{-1/2} F^{1/2} \tag{24}$$

   The last equation is similar to Eq. (11) with $B = 1/(A_c v_0)$ in $\mathrm{ml}^{-1/2}\mathrm{min}^{1/2}$.
2. The mobile phase is dispersed into small droplets in mixing cycles.

   For Eq. (12) we have in this case $S_d = 1 - S_f$, $F_c = 0$, $F_d = F$ and

$$\frac{F}{A_c(1-S_f)} = S_f v_0 \quad \text{or} \quad S_f(1-S_f) = \frac{F}{(A_c v_0)}$$

3. Experimental

A full account of the experimental set-up and experiment procedure is given elsewhere [5]. For clarity the description of the apparatus, phase system and sample system is repeated here.

3.1. Apparatus

A new Milli-CCC® instrument, with a rotor radius of $R = 50$ mm, speed range $\omega = 500$–2100 rpm ($g = 14$–247) with temperature controlled to $+1\,^{\circ}$C from 20 to 30 °C, was used for all the experimental work. The coil was wound from stainless steel with a $d = 0.76$ mm bore, coil volume $V_c = 4.6$ ml and inlet/outlet leads volume $V_{ext} = 0.3$ ml giving a total system volume of $V_t = 4.9$ ml. The total coil length $L = 10.2$ m with 44 loops and β range of 0.68–0.79. The coil is wound from head (centre) to tail (periphery) when rotating clockwise.

3.2. Phase system

A heptane/ethyl acetate/methanol/water (1.4:0.6:1.0:1.0) phase system was used throughout this study. This is an intermediate phase system from the hydrophobicity point of view with a relatively high density difference between the phases ($\rho_s = 0.708\,\mathrm{g/cm^3}$, $\rho_m = 0.938\,\mathrm{g/cm^3}$), a significant viscosity difference between the two phases ($\eta_s = 0.35$ cP and $\eta_m = 1.35$ cP) and a relatively low interfacial tension ($\tau_i = 6.2$ mN/m).

3.3. Sample system

Chemically pure organic solvents were applied without additional treatment. Uracil (2,4-dixydroxypyrimidine, 99%, Sigma) was used as a $K_D = 0$ marker peak. The chosen test system was benzyl alcohol (99%, Sigma) and *p*-cresol (4-methylphenol, 99%, Sigma). The sample was injected in the column using a Rheodyne injection loop of 50 μl volume (1% of coil volume V_c).

4. Results and discussion

Two sets of experiments were performed: the first set was carried out under constant rotation speed ($\omega = 1800$ rpm) and varying mobile phase flow rate (Table 1), and the second one for constant flow rate ($F = 0.593$ ml/min) and different rotation speeds (Table 2). Two approaches were used to estimate S_f and K_D. (1) Direct measure of the volume of each phase after column emptying at the end of the run to estimate S_f and then K_D calculation from Eqs. (18)–(21); (2) calculation of S_f from Uracil peaks taking $K_D = 0.31$ and calculation K_D for the two other substances using the estimated values of S_f. The second method has lead to better results expressing in less deviation of K_D values for Uracil and benzyl alcohol. These results are given in the tables. The number of cells was determined by using two methods discussed above.

4.1. Axial mixing in the phases

As can be seen from Tables 1 and 2, the values of n obtained by using the peak base width (Eq. (22)) considerably differ from those found by using peak height (Eq. (23)). Comparing the values of n found by the two methods we can conclude that base width measurements are more susceptible to experimental errors (because of some uncertainty in drawing tangents) than peak height measurements which take into calculation somewhat the whole curve (Eq. (23)).

The measured values of elution time τ_{max} are slightly lower than the values of mean residence time calculated from chromatograms by using the first moment (Eq. (19)). This fact is in good agreement with the theory: the position of the peak maximum at the time axis can be found from Eq. (8) in non-dimensional form:

$$t_{max} = \frac{n-1}{np} \tag{25}$$

or in real time

$$\tau_{max} = \frac{V_c}{F}\frac{n-1}{np} = \frac{n-1}{n}\frac{V_c}{F}(1 - S_f + S_f K_D) \tag{26}$$

From Eqs. (20) and (26) we have: $\bar{\tau} > \tau_{max} = \tau_R$; for $n \to \infty$, $\tau_R = \bar{\tau}$.

Fig. 2a shows the plot of $1/n$, obtained by using Eq. (23), versus K_D as predicted in Eq. (17) for the first set of experiments (Table 1). The results for the second set are presented in Fig. 2b. For constructing the diagrams the average value of distribution constant K_D for each peak was used. The rates of longitudinal mixing D_{axm} and D_{axs} can be obtained from the intercept and slope of the linear regressions in Fig. 2. These results are shown in Tables 3 and 4. They demonstrate

Table 1
Experimental data obtained for the constant rotation speed ($\omega = 1800$ rpm)

Sample	F (ml/min)	S_f	$\bar{\tau}$ (min)	τ_{max} (min)	K_D (Eq. (21))	n (Eq. (22))	n (Eq. (23))
Uracil	0.30	0.920	5.97	5.80	0.31	240	180
	0.60	0.872	3.25	3.15	0.31	250	200
	1.09	0.798	2.02	1.97	0.31	400	280
	1.50	0.726	1.63	1.60	0.31	450	260
	2.00	0.668	1.32	1.30	0.31	650	370
Benzyl alcohol	0.30	0.920	9.14	9.05	0.521	240	190
	0.60	0.872	4.76	4.70	0.522	260	190
	1.09	0.798	2.79	2.75	0.525	290	220
	1.50	0.726	2.15	2.12	0.529	320	190
	2.00	0.668	1.68	1.65	0.53	370	250
p-Cresol	0.30	0.920	18.0	17.9	1.11	230	180
	0.60	0.872	8.87	8.80	1.10	160	140
	1.09	0.798	4.83	4.80	1.10	140	130
	1.50	0.726	3.50	3.45	1.10	140	100
	2.00	0.668	2.62	2.55	1.10	150	130

Table 2
Experimental data obtained for the constant flow rate ($F = 0.590$ ml/min)

Sample	ω (rpm)	S_f	$\bar{\tau}$ (min)	τ_{max} (min)	K_D (Eq. (21))	n (Eq. (23))	n (Eq. (22))
Uracil	900	0.535	5.21	5.20	0.31	750	610
	1200	0.714	4.19	4.16	0.31	420	340
	1500	0.820	3.59	3.52	0.31	270	220
	1800	0.879	3.25	3.15	0.31	270	250
	2100	0.893	3.17	3.10	0.31	260	240
Benzyl alcohol	900	0.535	6.34	6.25	0.565	530	320
	1200	0.714	5.57	5.50	0.544	320	240
	1500	0.820	5.10	5.05	0.533	260	250
	1800	0.879	4.90	4.80	0.537	250	200
	2100	0.893	4.89	4.80	0.543	260	200
p-Cresol	900	0.535	8.74	8.70	1.11	200	160
	1200	0.714	8.94	8.85	1.11	160	150
	1500	0.820	9.02	8.90	1.11	150	130
	1800	0.879	9.15	8.95	1.12	150	130
	2100	0.893	9.21	9.10	1.13	170	160

Table 3
Parameters of axial mixing calculated from Fig. 2 (constant rotation speed, $\omega = 1800$ rpm)

No.	u (cm/s)	S_f	D_{axm} (cm^2/s)	D_{axs} (cm^2/s)	$K_D = 0.31$		$K_D = 0.525$		$K_D = 1.1$	
					n exp.	n calc.	n exp.	n calc.	n exp.	n calc.
1	1.10	0.920	27.9	0.24	240	240	240	240	230	220
2	2.20	0.872	22.5	4.06	250	280	260	230	160	160
3	4.01	0.798	5.0	15.0	400	430	290	280	140	140
4	5.52	0.726	0.62	24.1	450	500	320	300	140	140
5	7.36	0.668	0	34.8	650	510	370	300	150	140

Table 4
Parameters of axial mixing calculated from Fig. 2 (constant flow rate, $F = 0.59$ ml/min)

No.	ω (rpm)	S_f	D_{axm} (cm^2/s)	D_{axs} (cm^2/s)	$K_D = 0.31$		$K_D = 0.544$		$K_D = 1.12$	
					n exp.	n calc.	n exp.	n calc.	n exp.	n calc.
1	900	0.535	0	9.46	750	700	530	400	200	190
2	1200	0.714	2.69	7.40	420	460	320	300	160	160
3	1500	0.820	12.8	5.37	270	300	260	230	150	150
4	1800	0.879	20.0	4.88	270	290	250	230	150	150
5	2100	0.893	27.8	3.33	260	280	260	240	170	170

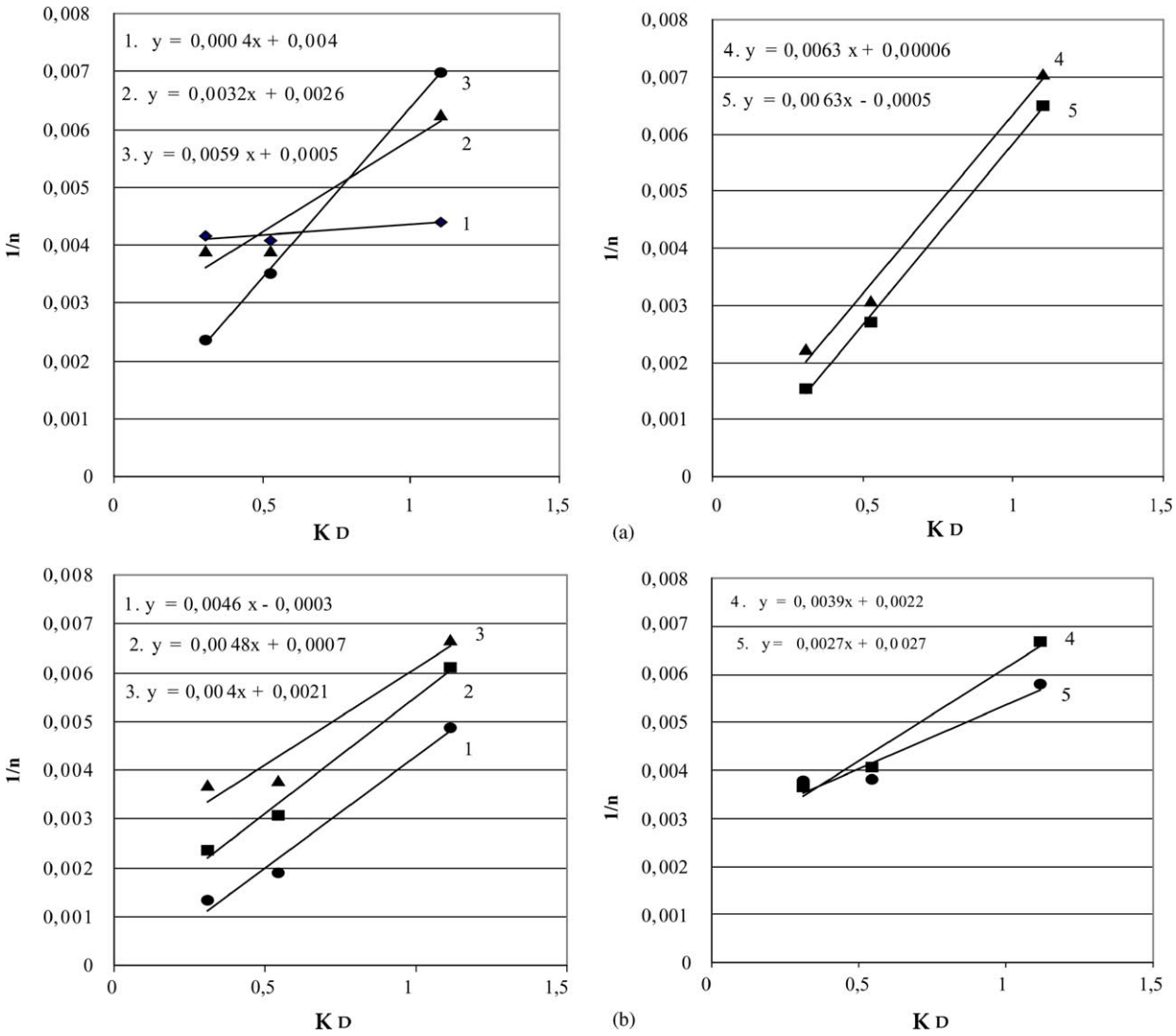

Fig. 2. Inverse value of cell number vs. distribution constant for the first (a) and second (b) set of experiments. Plot numbers correspond to experiment numbers in Tables 3 and 4.

that with increasing volume fraction of each phase in the tubing the rate of axial mixing in the corresponding phase decreases. The values of cell number determined from the experimental peak heights are compared in Tables 3 and 4 with n calculated from estimated S_f, K_D, D_{axs} and D_{axm} by using Eq. (13). As can be seen from the tables there is a good agreement between the experimental and calculated values of cell number, except for plots where a negative intercept was obtained, where the value of D_{axm} was taken to be zero. The negative values of intercept are observed for the lowest stationary phase retention ratio, S_f, that is for either the highest flow rate (Table 3) or the lowest rotation speed (Table 4). This discrepancy may be explained by a possible slow interphase mass transfer in these experiments (due to reduced contacting time in the first case, and reduced contacting area in the last one) so that the equilibrium could not be fully achieved.

In Figs. 3–5 the peak profiles of the original chromatograms are compared with those simulated by Eqs. (8) and (9) using the experimental values of S_f, K_D, Q, V_c, F and n. The results in Figs. 3–5 demonstrate in general a fair agreement between the experimental and calculated data. The model corresponds best with the last-eluted peak shape, then to the second-eluted peak shape. Maximum deviation is observed for the first-eluting peak. The amount (Q) of the first solute was the smallest and that for the last solute, the largest: the ratio of solute amounts in each sample were on average: $Q_1{:}Q_2{:}Q_3 = 1{:}2{:}4$. When small amounts of a solute are injected the peak shapes are highly dependent on the injection conditions and experimental errors.

Fig. 5 (last-eluted peaks) shows that for the cell number $n < 200$ Eq. (8) describes experimental curves better than Eq. (9). For $n > 200$ the rigorous solution (8) and the approximation (9) give practically identical results (Fig. 4).

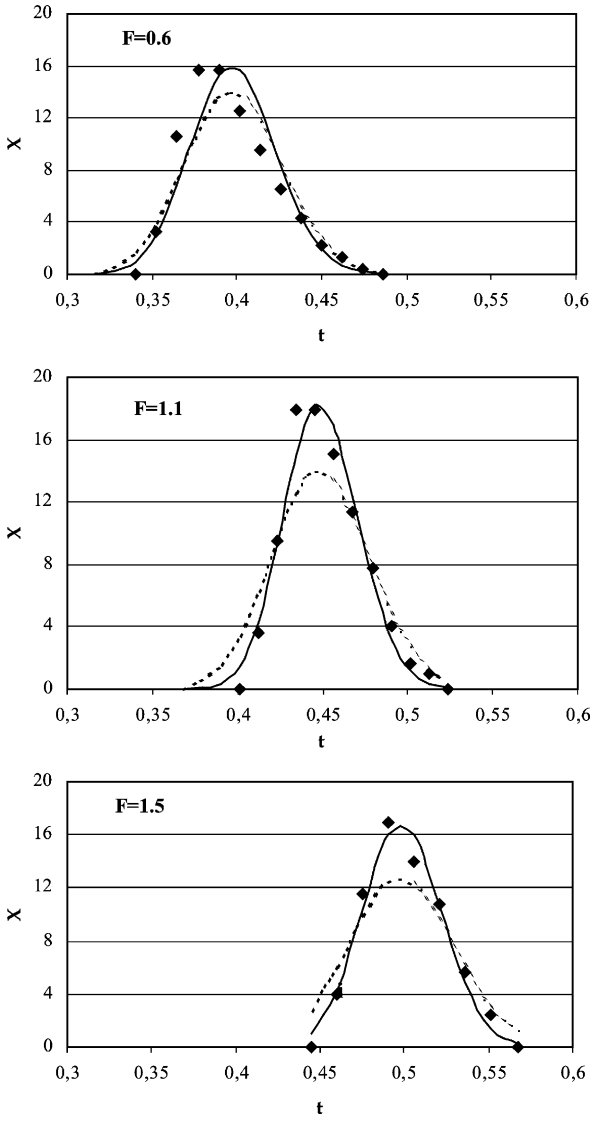

Fig. 3. Comparison of experimental peaks (points) and peaks generated by using Eq. (8) with n determined by Eq. (23): solid line; and Eq. (22): dotted line, for Uracil, the first-eluted solute.

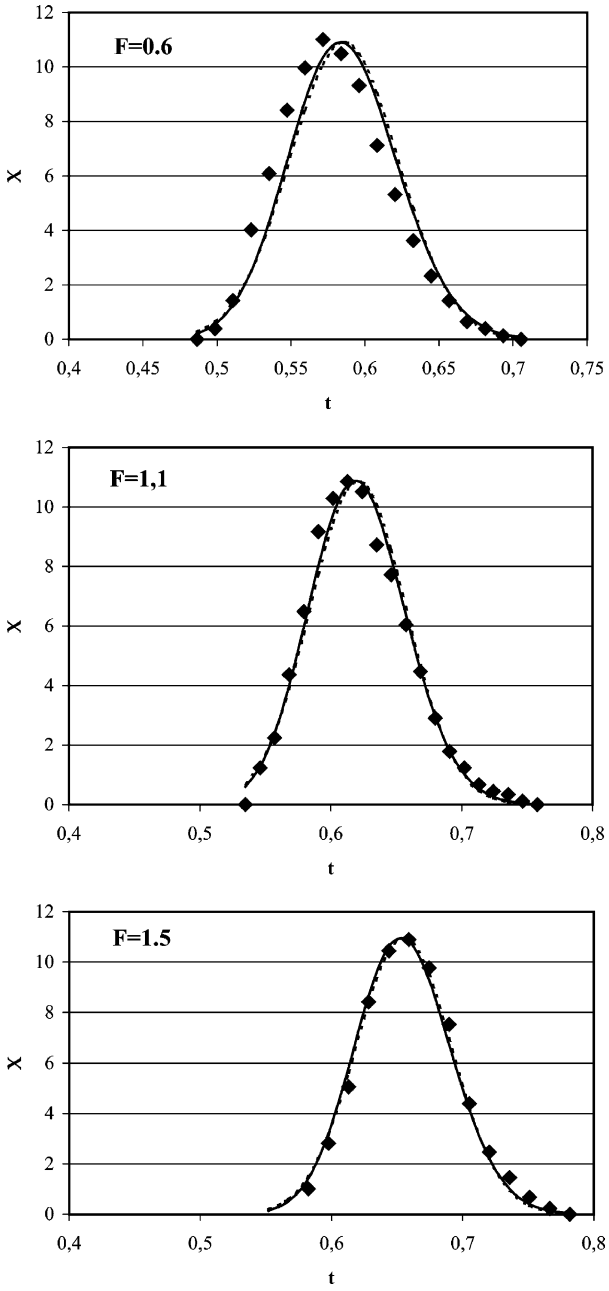

Fig. 4. Comparison of experimental peaks (points) and peaks generated by using Eq. (8): solid line; and Eq. (9): dotted line, for benzyl alcohol, the second-eluted solute.

Thus, using Eqs. (8) and (13) we can predict the chromatographic behaviour of solutes if the experimental data for some other solutes are known.

The above interpretation of chromatographic peaks is based on assumption of a very rapid mass transfer (limiting case 2 in Section 1.1). To prove it, further investigations are to be done; it is necessary to determine the real contribution of mass transfer and axial mixing into band broadening.

4.2. Stationary phase retention volume

A linear relationship between the square root of the flow rate and the retention of the stationary phase was obtained with r^2 parameters higher than 0.97 in all studied cases. This result validates Eq. (24). Thus, a conclusion could be drawn. If assumption 1 in Section 2.2. is valid, the stationary phase is dispersed into small droplets in mixing cycles. Nevertheless, it cannot to be excluded that high mass transfer rates in CCC are achieved by other forms of interface building (for instance, by wave building) and/or due to intense turbulence decreasing the resistance to interphase mass transfer in the phases. In addition, considering the droplets building it may be expected that the stationary phase will be the dispersed phase when $S_f < 0.5$, with a continuous mobile phase. When $S_f > 0.5$ the mobile phase will be the dispersed phase in a continuous stationary phase. Irrespective of interphase building mechanism, the physical

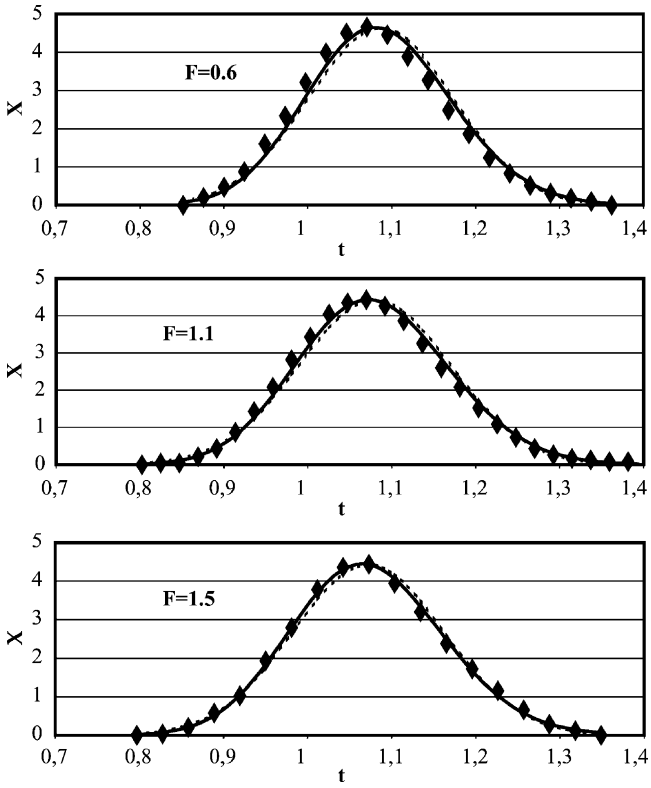

Fig. 5. Comparison of experimental peaks (points) and peaks generated by using Eq. (8): solid line; and Eq. (9): dotted line, for *para*-cresol, the last-eluted solute.

interpretation of Eq. (24) in form:

$$\frac{F}{A_c(1-S_f)} = (1-S_f)v_0$$

could be the true mobile phase linear velocity is equal to a characteristic velocity v_0 multiplied by the hindering factor $(1-S_f)$. The characteristic velocity can be considered as mobile phase velocity when $S_f \to 0$, or $V_s \to 0$. It can also be view of the velocity of a mobile phase droplet in the liquid stationary phase. Such velocity obeys the Stokes law that defines v, the velocity of a hard sphere of radius, r, in a liquid system of viscosity, η, submitted to a field, G, as:

$$v = \frac{2r^2\Delta\rho G}{9\eta} \quad (27)$$

in which $\Delta\rho$ is the phase density difference and G can be roughly estimated as $\omega^2 R$, the centrifugal field. A linear relationship between the characteristic velocity of mobile phase, v_0, and the square of rotation speed, ω^2, was obtained with a regression coefficient of 0.975.

5. Conclusion

Experiments were carried out to prove the effectiveness of the cell model to predict partitioning behaviour and the chromatographic peak profiles of solutes. It is shown that the equilibrium cell model (Eq. (8)) is particularly suitable for describing CCC chromatographic peaks. The comparison of original chromatograms with theoretical curves generated by the considered model has demonstrated a satisfactory agreement between them. Longitudinal mixing rates in stationary and mobile phases can be experimentally determined by using several peaks of a sample, which enables the peak shape for a solute with a given distribution constant to be predicted from experimental data from other solutes.

A physical interpretation of the relationship between stationary phase retention and the square root of mobile phase flow rate is suggested.

6. Nomenclature

A_c	CCC column cross-sectional area (cm^2)
B	slope of the S_f versus square root of the mobile phase flow rate lines ($min^{1/2}\,cm^{2/3}$)
D_{axm}	longitudinal diffusion coefficient of the solute in the mobile phase (cm^2/s)
D_{axs}	longitudinal diffusion coefficient of the solute in the stationary phase (cm^2/s)
F	mobile phase flow rate (ml/min or cm^3/s)
F_c	flow rate of the continuous phase in extraction columns (ml/min or cm^3/s)
F_d	flow rate of the dispersed phase in extraction columns (ml/min or cm^3/s)
K_D	solute distribution constant, $= y/x$
L	length of tubing making the CCC column (cm)
n	number of ideally mixed cells in the CCC column
n_c	number of perfectly mixed cells in the case of $S_f = 0$ (one liquid phase in the column)
P	dimensionless integration parameter, $= V_c/V_R$
Pe	Peclet number (linked to axial mixing, see Eq. (6))
Q	amount of solute injected (in moles or grams)
S_d	dispersed phase holdup in extraction columns, equivalent to S_f in CCC
S_f	the liquid stationary phase retention ratio, $= V_s/V_c$
t_{max}	retention time at peak maximum (s)
u	velocity of a $K_D = 1$ solute, $= F/A_c$ (cm/s)
v_0	droplet velocity in extraction columns (cm/s)
V_c	CCC column volume (ml)
V_m	volume of the mobile phase in the CCC volume (ml)
V_s	volume of the stationary phase in the CCC volume (ml)
W_b	peak width at base(s)
x	solute concentration in the mobile phase (M)
x_L	solute concentration in the mobile phase at a distance in the tubing (M)
x_n	solute concentration in cell number n (M)
$\bar{x}$	mean solute concentration in the column, $= Q/V_c$ (M)
y	solute concentration in the stationary phase (M)
z	longitudinal variable along CCC tubing (cm)

Greek

λ dimentionless number for matter dispersion, $= yD_{axs}/xD_{axm}$
τ integration variable for time (s)
τ_c mean residence time for a $K_D = 1$ solute, $= L/u$ (s)
τ_m $K_D = 0$ solute retention time, $= V_m/F$ (s)
τ_R solute retention time, $= V_R/F$ (s)
$\bar{\tau}$ mean solute residence time (s)
ω rotation speed of the CCC rotor (rad/s)

Acknowledgements

The authors are grateful to the EU INTAS programme no. 00-0782 entitled “Fundamental Research into the Hydrodynamics and Efficiency of Counter-Current Chromatography” and to the Russian President, grant no. NSH-1577.2003.3, for the financial support of this work.

References

[1] W.D. Conway, Countercurrent Chromatography: Apparatus, Theory and Applications, VCH Publishers Inc., New York, 1990.
[2] J.M. Menet, D. Thiebaut (Eds.), Countercurrent Chromatography, Chromatographic Science Series 82, Marcel Dekker Inc., Basel, New York, 1999.
[3] O. Bousquet, A.P. Foucault, F. Le Goffic, J. Liq. Chromatogr. 14 (1991) 3343.
[4] I.A. Sutherland, L. Brown, S. Forbes, D. Games, D. Hawes, K. Hostetmann, E.H. McKerrell, A. Marston, D. Wheatley, P. Wood, J. Liq. Chromatogr. Related Technol. 21 (1998) 279.
[5] I.A. Sutherland, in: J. Cazes (Ed.), Encyclopaedia of Chromatography, Marcel Dekker Inc., New York, 2001, p. 734.
[6] L. Marchal, A.P. Foucault, G. Patissier, J.M. Rosant, J. Legrand, in: A. Berthod (Ed.), CCC, The Support-Free Liquid Stationary Phase, Comprehensive Analytical Chemistry, vol. 38, Elsevier, Amsterdam, 2002 (Chapter 5).
[7] V.B. Di Marco, G.G. Bombi, J. Chromatogr. A 931 (2001) 1.
[8] A.E. Kostanian, J. Chromatogr. A 973 (2002) 39.
[9] J. Villermaux, D. Schweich, M. Sardin, in: G. Ganestos, P.E. Barker (Eds.), Preparative and Production Scale Chromatography, Marcel Dekker, New York, 1992.
[10] J. Villermaux, in: A.E. Rodrigues, D. Tondeur (Eds.), Percolation Proceses: Theory and Applications, Sijthoff and Noordhoof.
[11] A.E. Dukler, Y. Taitel, in: J.M. Delhaye, N. Zuber (Eds.), Multiphase Science and Technology, vol. 2, Springler-Verlag, Berlin, 1986.
[12] A.S. Said, Theory and Mathematics of Chromatography, Huthig, New York, 1981.
[13] D. Schweich, M. Sardin, J. Hydrol. 50 (1981) 1.
[14] Q. Du, C. Wu, G. Qian, P. Wu, Y. Ito, J. Chromatogr. A 835 (1999) 231.
[15] D. Logsdail, L. Lowes, in: C. Hanson (Ed.), Recent Advances in Liquid–Liquid Extraction, Pergamon Press, Oxford, 1971.